Jordanian Journal of Engineering and Chemical Industries

Print ISSN: 2616 - 9584 Online ISSN: 2617 - 720X

Influence of *Bauhinia tomentosa* Stem Bark Extract on the Electrochemical Behavior of Low-Carbon Steel in 1 M HCl

Msenhemba Moses Mchihi*[1], Shonola Rebecca Ibukunola[2], Bilqis Omobola Seriki[1], Adeyinka Olubunmi Eruola[1], Aderibigbe Tajudeen Adejare[3], Paula Hembadoon Ado[1] and Opeolu Sunday Olutunji[1]

[1]Yaba College of Technology, School of Science, Department of Chemical Science, P. M. B. 2011, Yaba - Lagos, Nigeria
[2]Yaba College of Technology Lagos, School of Technical Education, Department of Science Education, P. M. B. 2011, Yaba - Lagos, Nigeria
[3]Yaba College of Technology Lagos, School of Science, Department of Science Laboratory Technology, P. M. B. 2011, Yaba - Lagos, Nigeria

Abstract

Plant-derived extracts serve as effective environmentally friendly inhibitors of corrosion because they are biodegradable, innocuous, and derived from renewable resources, rendering them a more friendly and sustainable substitute for harmful synthetic inhibitors. In this study, the inhibitive performance of *Bauhinia tomentosa* (BT) stem bark extract on low-carbon steel (L-CS) deterioration in 1 M hydrochloric acid was assessed via open circuit potential (OCP), potentiodynamic polarization (PDP), electrochemical impedance spectroscopy (EIS), and gas chromatography–mass spectrometry (GC–MS). The results show that BT extract suppressed L-CS corrosion, with inhibition efficiency improving as inhibitor concentration increases. Polarization data indicate that BT functions as a mixed-type inhibitor by simultaneously retarding anodic metal deterioration and cathodic hydrogen liberation reactions. Corrosion current density (I_{corr}) noticeably reduced from 1241 μAcm^{-2} (in the absence BT) to 687 μAcm^{-2} (in the presence of 1000 ppm of BT). Impedance measurements revealed improved resistance associated with charge transfer (R_{ct}), confirming adsorption of BT molecules on the L-CS exterior. R_{ct} increased from 3533 Ω cm^2 (without BT) to 4794 Ω cm^2 (when 1000 ppm of BT was introduced). GC–MS analysis identified organic compounds containing heteroatoms and pi-electron schemes, which enable robust interaction with the metal surface. An inhibition efficiency of up to 45% was achieved at 1000 ppm BT from PDP analysis, highlighting the prospect of BT extract as a corrosion inhibitor with modest performance in acidic environments.

Paper type: Research Paper

Keywords: Mild steel, HCl, Plant extract, Electrochemical techniques, Green corrosion inhibitor

Citation: Mchihi, M., M., Ibukunola, S., R., Seriki, B., O., Eruola, A., O., Adejare, A., T., Ado, P., H., and Olutunji, O., S. " Influence of *Bauhinia tomentosa* Stem Bark Extract on the Electrochemical Behavior of Low-Carbon Steel in 1 M HCl" *Jordanian Journal of Engineering and Chemical Industries*, Vol. **9**, No.1, pp:77-89 (2026).

1. Introduction

Low carbon steel (L-CS) continues to be one of the most commonly employed materials in engineering due to its affordability and advantageous mechanical characteristics. Even so, during various industrial procedures, specifically, removal of impurities from metal exterior using acid, and acidification in oil wells (Chioma et al., 2022), L-CS is often subjected to harsh acidic environments, such as H_2SO_4 and HCl, leading to accelerated deterioration of the material (El-Housseiny et al., 2022; Mchihi et al., 2025a). Consequently, the application of deterioration inhibitors becomes crucial for reducing metal loss and prolonging the durability of equipment (Al-

* Corresponding author: E-mail: *mosesmsenhemba@gmail.com* and *msenhemba.mchihi@yabatech.edu.ng* ORCID: **0000-0002-3815-6073**
Received: 12/Feburary/2026 Revised: 13/March/2026

Jordanian Journal of Engineering and Chemical Industries (JJECI), Vol.9, No.1, 2026, pp: 77-89 Accepted: 14/March/2026

Moubaraki et al., 2022; Mchihi et al., 2025b; Odozi et al., 2024). The mechanism by which these corrosion inhibitors interact at the metal-solution interface can be characterized by the formation of three distinct types of films: passivating films, precipitation films, and adsorption films (Thacker & Ram, 2025). The establishment of passivating films is better exemplified by traditional inorganic inhibitors, including chromates, which show a halting influence specifically in aerated solutions. In contrast, precipitation films produced by deterioration inhibitors are typically porous and do not adhere completely. These films arise from chemical species that generate insoluble coatings through reactions with either soluble species present in the corrosive medium or with ions of the metal being protected. Adsorption films are primarily constituted by organic compounds (Thacker & Ram, 2025).

While traditional inhibitors demonstrate effectiveness, they are frequently associated with disadvantages, including toxicity, inadequate biodegradability, and resistance to environmental degradation. In light of increasingly stringent environmental regulations, a rising emphasis on the exploration of plant-based deterioration inhibitors, which are renewable, biodegradable, and eco-friendly has been recorded (Verma et al., 2021; Mchihi et al., 2025b). Quite a lot of researchers have documented the efficacy of diverse plant-derived extracts as inhibitors for deterioration of diverse metals in different media (Mungwari et al., 2025; Odozi et al., 2021; Miralrio et al., 2020; Odozi et al., 2019; Emesiani et al., 2024; Mahraz et al., 2025; Mchihi et al., 2023; Meena et al., 2024). Some of the plants whose corrosion inhibition potential have been reported include *Artemisia argyi* (Chu et al., 2025), *Chrysanthemum indicum* (Chu et al., 2025), *Gnetum africanum* (Obiukwu et al., 2015), *Schinopsis lorentzii* (Gerengi and Sahin, 2011), *Gongronema latifolium* (Obiukwu et al., 2015), *Euphorbia hirta* (Nnanna et al., 2010), *Dialum guineense* (Nnanna et al., 2010), *Pennisetum purpureum* (Ituen et al., 2016), *Eriobotrya japonica Lindl*. (Zheng et al., 2018), *Garcinia Cambogia* (Rani et al., 2022), and *artabotrys odoratissimus* (Rathod et al., 2022). A good number of these plants demonstrated high efficiency of inhibition while few showed low inhibition efficiency. The application of extracts rich in phytochemicals as deterioration inhibitors presents numerous advantages, including economic viability, environmental sustainability, abundant availability, and straightforward production methods (Thacker and Ram, 2025). Plant extracts generally comprise intricate mixtures of organic compounds, including phenolics, flavonoids, alkaloids, and terpenoids, which add to their inhibitory properties, via adsorption onto metal surfaces through heteroatoms and conjugated π-electron systems (Eddy et al., 2015).

Literature indicates that several parts of *Bauhinia tomentosa* (BT) are rich in bioactive compounds that are capable of creating a protective barrier on metal surfaces, thereby reducing metal deterioration (Kumar et al., 2025; Balabhaskar and Vijayalakshmi, 2015). A study utilized an extract from the leaves of BT as an inhibitor for L-CS deterioration in a 1 M HCl solution, attaining a highest inhibition efficiency of 93.47% at 308 K when 700 ppm of the leaf extract was present (Perumal et al., 2017). Despite the growing number of studies on green inhibitors, research exploring the inhibitory properties of extracts from other parts of the plant (BT), such as the stem bark, appears to be limited. Specifically, information on the corrosion inhibition capability of BT stem bark extract on L-CS deterioration in hydrochloric acid remains scarce. This effort aims to assess the inhibitory impact of BT stem bark extract for L-CS deterioration in 1 M HCl.

2. Materials and Methods

2.1 Extraction

The extraction protocol described by Odozi et al. (2024) was followed to prepare the BT stem bark extract. Fresh BT stem bark were air-dried and milled into a fine powder with an electric blender. Approximately 20 g of the powdered BT was soaked in 250 mL of methanol in sealed sample container and agitated thoroughly to ensure proper mixing. The resulting mixture was sonicated for 10 minutes to enhance extraction efficiency. Subsequently, the mixture was subjected to filtration, and the filtrate was centrifuged for 5 minutes to remove any remaining particulates. An aliquot of the clarified BT extract was reserved for GC-MS analysis, while the remainder was concentrated with a rotary evaporator and employed to prepare various dosages of the inhibitor (Odozi et al., 2024).

2.2 Gas Chromatrography-Mass Spectrometry (GC-MS)

The chemical constituents of the BT stem extract were characterized using an Agilent 5977B GC/MSD scheme attached to an Agilent 8860 automatic sampler in accordance with the procedure described in a previous study (Mchihi et al., 2024b). Separation was achieved on an Elite-5MS capillary column (5% diphenyl/95% dimethyl polysiloxane) with dimensions of 30 m × 0.25 mm internal diameter and 0.25 μm film thickness. High-purity helium (99.9%) assisted as the carrier gas at a steady flow rate of 1 mL min^{-1}. A sample volume of 1 μL was inserted using a split mode with a ratio of 10:1. Ionization was carried out via electron impact (EI) at 70 eV. The injector temperature was maintained at 300 °C, while the temperature of the source of ion was set at 250 °C. The oven temperature program commenced at 100 °C (held for 0.5 min), followed by a ramp of 20 °C min^{-1} to 280 °C, where it was held for 2.5 min. Mass spectra were recorded at 70 eV with a scan interval of 0.5 s across a mass-to-charge (m/z) range of 45–450 Da. A solvent delay of 0–180 s was applied, and the total analysis time was 21.33 min.

2.3 Electrochemical Investigation

Electrochemical measurements were conducted using a conventional 3-electrode configuration involving a Pt wire, a L-CS specimen, and an Ag/AgCl electrode. The Pt wire functions to finalize the circuit, enabling the passage of electric current to the L-CS (which is the host for electrochemical reactions). The Ag/AgCl electrode serves a as reliable and consistent reference potential due to its stability and non-polarizable characteristics. The Experiments were performed using a Metrohm Autolab PGSTAT204 potentiostat/galvanostat. 1 M HCl solution served as the electrolyte medium. Prior to other electrochemical tests, the open circuit potential (OCP) of the L-CS was monitored to determine the steady-state (free corrosion) potential and to minimize capacitive current effects. Electrochemical impedance spectroscopy (EIS) tests were conducted over a frequency range of 100 kHz-10 mHz using an AC perturbation amplitude of 10 mV. The resistance associated with charge transfer (R_{ct}) values acquired from EIS were used to evaluate the inhibition efficiency (IE) according to Equation 1 (Mchihi et al., 2024a), where R_{ct} and R_{ct}^{0} represent the resistance associated with charge transfer in the presence and absence of BT, respectively. Potentiodynamic polarization (PDP) studies were conducted within a potential window of −250 mV to +250 mV relative to OCP at a scan rate of 0.2 mV s^{-1}. The experimental data were processed using ZsimpWin 3.2 software for EIS analysis and EC-Lab software for polarization measurements. The inhibition efficiency from PDP data was calculated using Equation 2 (Mchihi et al., 2025c), where $I°_{corr}$ and I_{corr} denote the corrosion current densities in the uninhibited and inhibited systems, respectively. Surface coverage (θ) values were subsequently determined using Equation 3.

$$IE = \frac{Rct - R^{0}ct}{Rct} \times 100 \quad (1)$$

$$IE = \frac{I°corr - Icorr}{I°corr} \text{ X } 100 \quad (2)$$

$$\theta = \frac{IE}{100} \quad (3)$$

3. Results and Discussion

3.1 Open Circuit Potential (OCP) Behavior

The time-dependent profiles (**Figure 1**) of OCP indicate that the incorporation of BT extract results in minor alterations in potential when compared to the uninhibited solution, suggesting that BT has an impact on the deterioration of L-CS in HCl (Mchihi et al., 2024b).

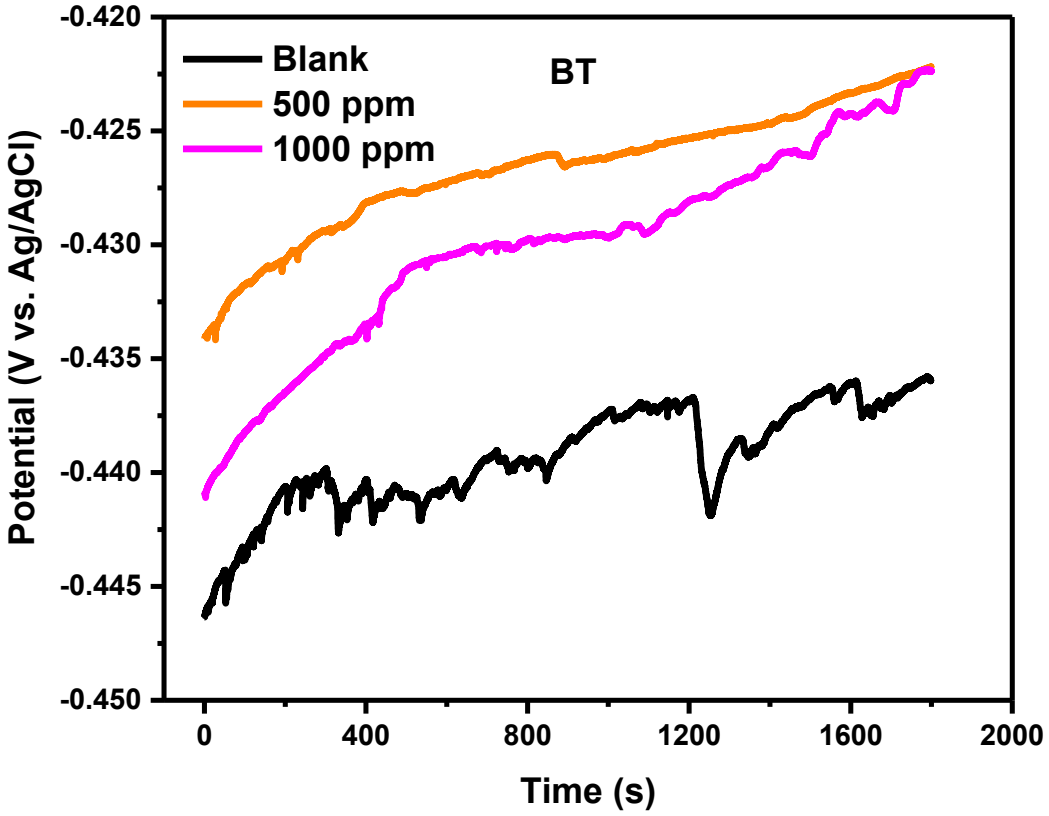

Fig. 1. OCP- time plots for L-CS in 1 M HCl without BT and in the presence of BT.

These alterations are insufficient to categorize BT as distinctly anodic or cathodic, implying a balanced effect on both electrochemical processes. The observed improvement in stabilization of potential over time suggests a gradual adhesion of BT molecules on the exterior of L-CS, ultimately enabling the establishment of a shielding BT film.

3.2 PDP Analysis

The polarization data and curves presented in **Table 1** and **Figure 2** revealed an extensive reduction in I_{corr} following the introduction of BT extract.

Table 1. PDP data for L-CS in HCl without BT and in the presence of BT

System	E_{corr} mV/Ag/AgCl	I_{corr} μAcm^{-2}	βa $mVdec^{-1}$	βc $mVdec^{-1}$	θ	IE %
Blank	-421	1241	41	88		
500 ppm	-425	968	52	61	0.22	22
1000 ppm	-415	687	66	57	0.45	45

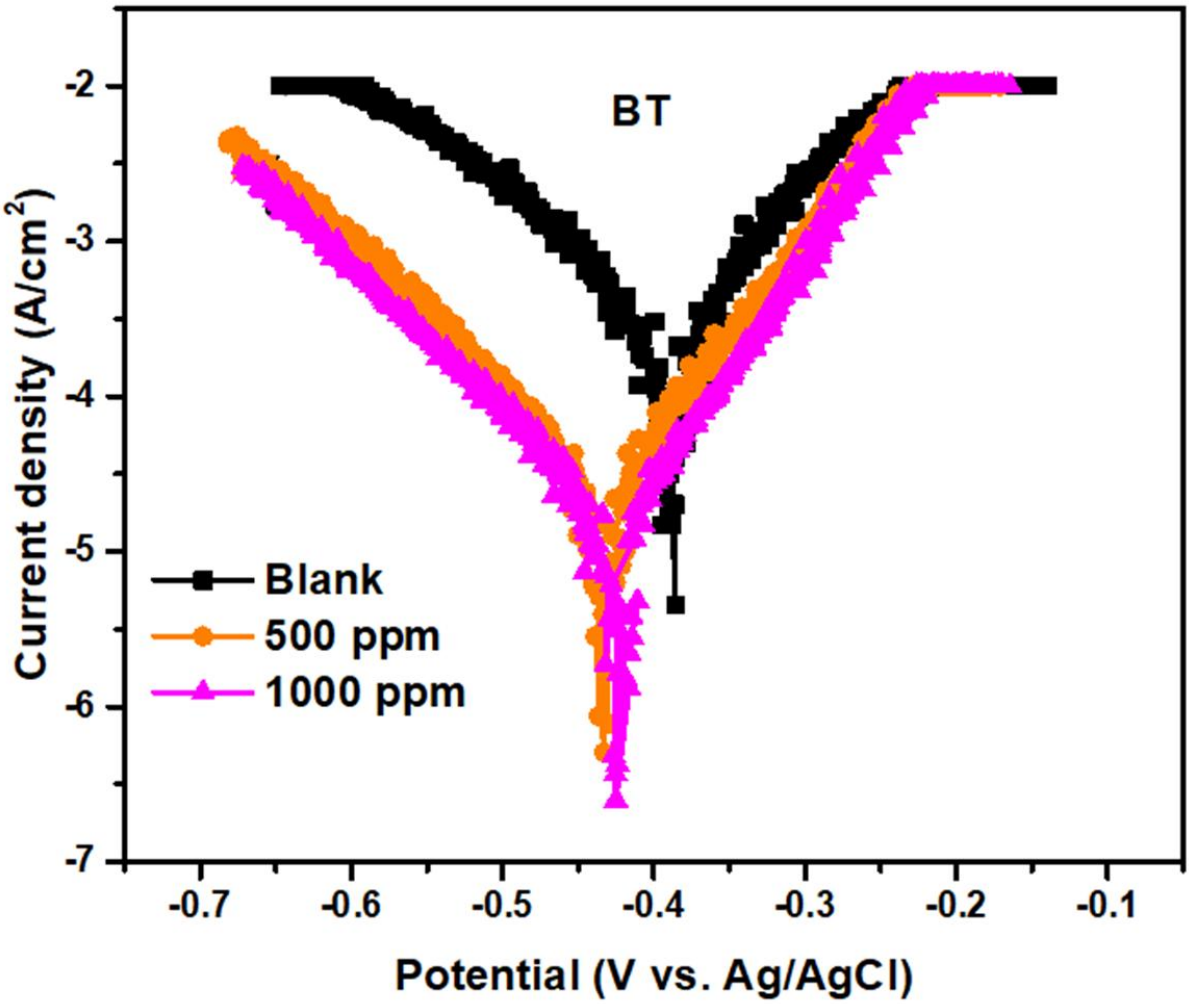

Fig. 2. Polarization plots for L-CS in 1M HCl without BT and in the presence of BT.

This reduction in I_{corr} improved consistently with greater dosage of the inhibitor, thereby affirming an enhancement in inhibition efficiency (Mchihi et al., 2024c). At a concentration of 1000 ppm BT, the I_{corr} is diminished by nearly 50% in comparison to the blank solution. Also, the corrosion potential shows only slight displacement in the presence of BT, revealing the mixed-type behavior of BT. This finding agrees with another study that reported the mixed-type inclination of BT leaves extract for deterioration of L-CS in HCl (Perumal et al., 2017). The alteration of both anodic and cathodic Tafel slopes suggests that BT extract plays a role in impeding the processes of dissolution and hydrogen evolution. Comparable electrochemical behaviors have been documented for inhibitors derived from plant sources that contain organic compounds rich in oxygen and nitrogen (El-Housseiny et al., 2022). The recorded efficiency of inhibition in this study is less than the efficiency reported in a study that employed BT leaves extract (Perumal et al., 2017). This may arise from difference in phytochemical content of stem bark and leaves of BT.

Despite numerous studies documenting the efficacy of extracts as deterioration inhibitors with high inhibition efficiencies, there are also findings concerning plant extracts that have demonstrated low inhibition efficiencies. In a study conducted by Gerengi and Sahin (2011), the corrosion inhibition of L-CS in a 1 M HCl environment was examined utilizing various concentrations of *Schinopsis lorentzii* extract. Their findings indicated an efficiency of inhibition of 31.7% at a dosage of 1000 ppm, as derived from EIS data. When the dosage of the inhibitor was increased to 2000 ppm, the efficiency of inhibition rose to 38.6%. It is important to note that certain plant extracts may exhibit limited corrosion inhibitory effects due to their low solubility in aggressive acidic environments and their complex (unrefined) compositions, which often lead to inadequate adhesion to metallic surfaces. Synergism is known to boost inhibition efficiency. A synergistic effect can be achieved by utilizing a combination of bark and leaf extracts, or by incorporating other compounds, which typically enhances efficiency. For instance, Aldahiri et al. (2025) demonstrated that the efficiency of inhibition of *Canarium strictum* leaf extract for mild steel in a 15% HCl solution was significantly improved by the addition of 5 ppm of potassium iodide (KI). Therefore, higher efficiency of inhibition could be achieved for BT stem bark through synergy.

Fazal et al. (2022) assert that achieving protection levels equivalent to those offered by traditional inhibitors often necessitates the use of high concentrations of inhibitors derived from plant extracts. While many of these plant-derived inhibitors effectively provide sufficient protection, there remains a pressing need for the optimization of these formulations. One effective approach to this optimization involves conducting phytochemical screenings along with computational simulations to isolate the most potent compounds among the several compounds found in a given extract. Subsequently, a thorough investigation of the synergistic interactions between these active molecules could be undertaken to develop a formulation that surpasses current standards. Also, it is important to note that most commercially available inhibitor formulations typically consist of a mixture of diverse chemical compounds (Fazal et al., 2022).

3.3 Electrochemical impedance spectroscopy (EIS) outcome

The electrical equivalent circuit engaged to fit EIS data is presented in **Figure 3**, while the plot generated from EIS measurements is illustrated in **Figure 4**.

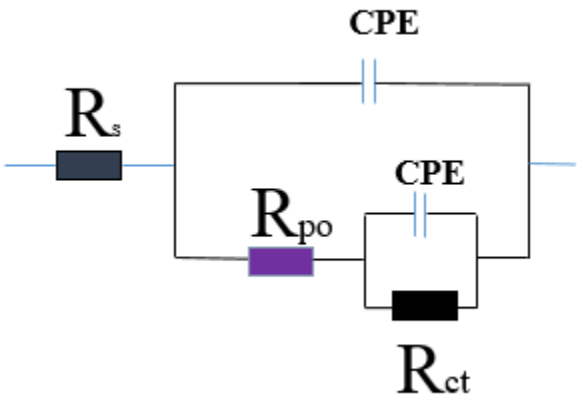

Fig. 3. Electrical equivalent circuit engaged for fitting EIS data.

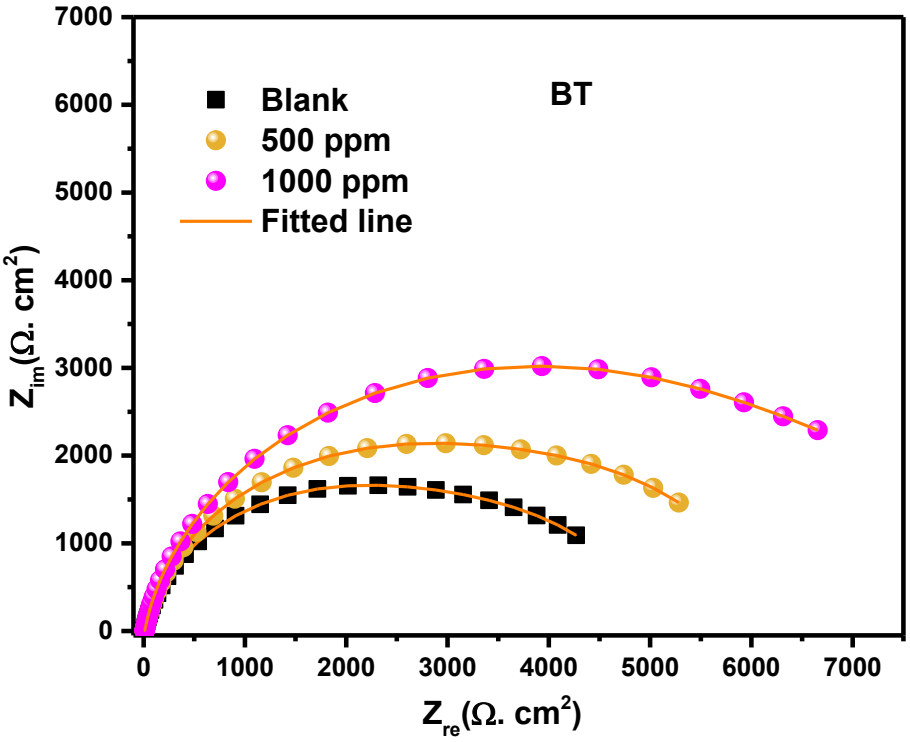

Fig. 4. Impedance plots for L-CS in 1 M HCl without and with different dosages of BT

In **Figure 3**, R_s symbolizes solution resistance, R_{po} denotes pore resistance, R_{ct} is the resistance associated with charge transfer and CPE is the constant phase element. The two Constant Phase Elements illustrate distinct, non-ideal capacitive behaviors owing to surface heterogeneity. R_{po} quantifies the resistance encountered by the electrolyte as it travels through the pores of a coating. R_{ct} indicates the resistance to electron transfer at the interface of the metal surface, reflecting the kinetics of the corrosion reaction. R_s denotes the ionic resistance presented by the electrolyte solution located between the working and reference electrodes, with a lower R_s signifying a cleaner electrolyte; it is typically minimal and may be regarded as a constant value. In this study, while the R_s values (**Table 2**) show very minimal variations, both R_{ct} and R_{po} values (**Table 2**) increased in the presence of BT, which suggests obstruction of some active sites and decrease in charge transfer (Aldahiri et al., 2025).

Table 2. EIS parameters for L-CS in bare HCl and BT enriched HCl

System	R_s (Ω cm^2)	R_{po} (Ω cm^2)	CPE1 ($\mu\Omega^{-1}$ s^n cm^{-2} X 10^{-5})	n1	R_{ct} (Ω cm^2)	CPE2 ($\mu\Omega^{-1}$ s^n cm^{-2} X 10^{-5})	n1	θ	IE %
Blank	10.5	1392	5.31	0.89	3533	5.90	0.85		
500 ppm	10.48	1465	5.12	0.89	4719	5.52	0.90	0.25	25
1000 ppm	10.5	2461	4.90	0.89	4794	3.30	0.96	0.47	26

The EIS plot exhibit single depressed semicircles, indicative of corrosion processes that are governed by transfer of charge. The surge in the diameter of the semicircle with greater concentrations of BT signifies an improvement in resistance associated with charge transfer as evident in **Table 2** (El-Housseiny et al., 2022). This trend is in agreement with other reports (Odozi et al., 2024). Quantitative impedance parameters reveal a noticeable rise in R_{ct} in solutions that have been inhibited (**Table 2**), along with a reduction in the values of the constant phase element. This phenomenon could be credited to the replacement of adsorbed H_2O molecules by components of BT and the establishment of a dense defensive film on the exterior of the L-CS. The two n values represent homogeneity factors for

CPE, quantifying surface roughness, non-ideality, or porous film properties. Values of n obtained in this study are less than 1. Ranging from 0 to 1, n=1 suggests an ideal capacitor, while lower values reflect surface heterogeneity.

The Bode phase angle and magnitude diagrams in **Figure 5** further corroborate the EIS outcomes.

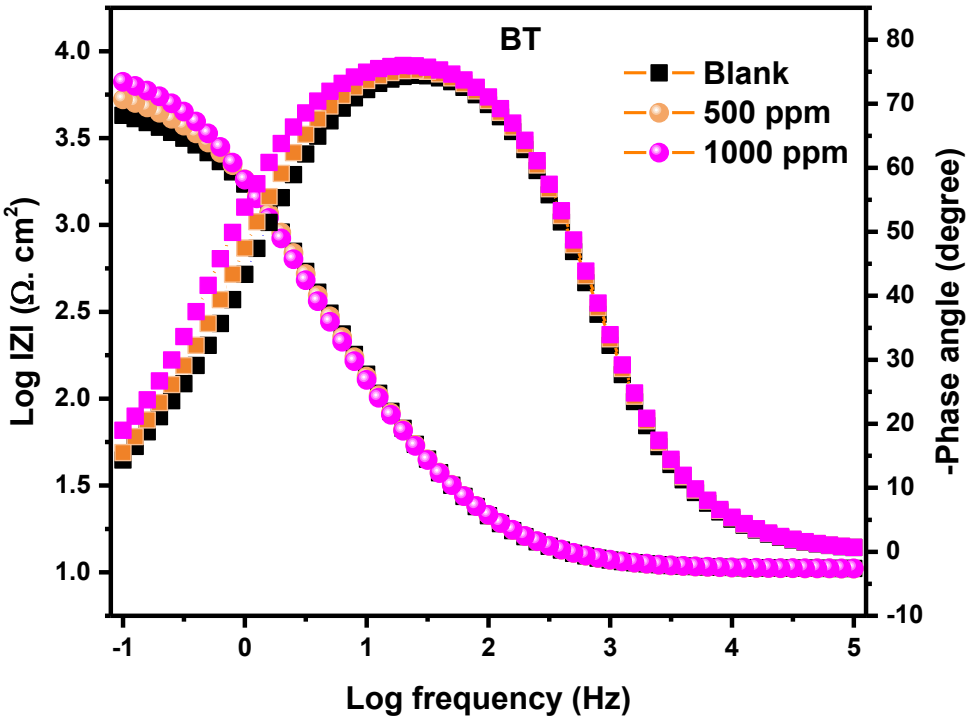

Fig. 5. Bode magnitude and phase angle for L-CS in HCl without BT and in the presence of BT.

In the Bode magnitude diagrams, introducing BT leads to a pronounced rise in the impedance modulus at the low-frequency region. This behavior signifies an increase in resistance and a suppression of the charge transfer reactions occurring on the L-CS interface (Mchihi et al., 2025b). Such an enhancement is attributed to the development of a defensive adsorbed layer that hinders L-CS dissolution. Meanwhile, the high-frequency domain shows minimal variation, indicating that the bulk solution resistance remains essentially unaffected by the incorporation of BT. Regarding the Bode phase angle plots, the incorporation of BT results in a higher maximum phase angle and a wide phase peak. This response reflects improved capacitive characteristics and a more uniform surface condition.

3.4 GC-MS

The GC–MS analysis of the stem bark extract from BT indicates a chemically varied composition, primarily consisting of oxygen-containing organic compounds, fatty acids, unsaturated hydrocarbons, and derivatives of carbohydrates as shown in **Figure 6** and **Table 3**.

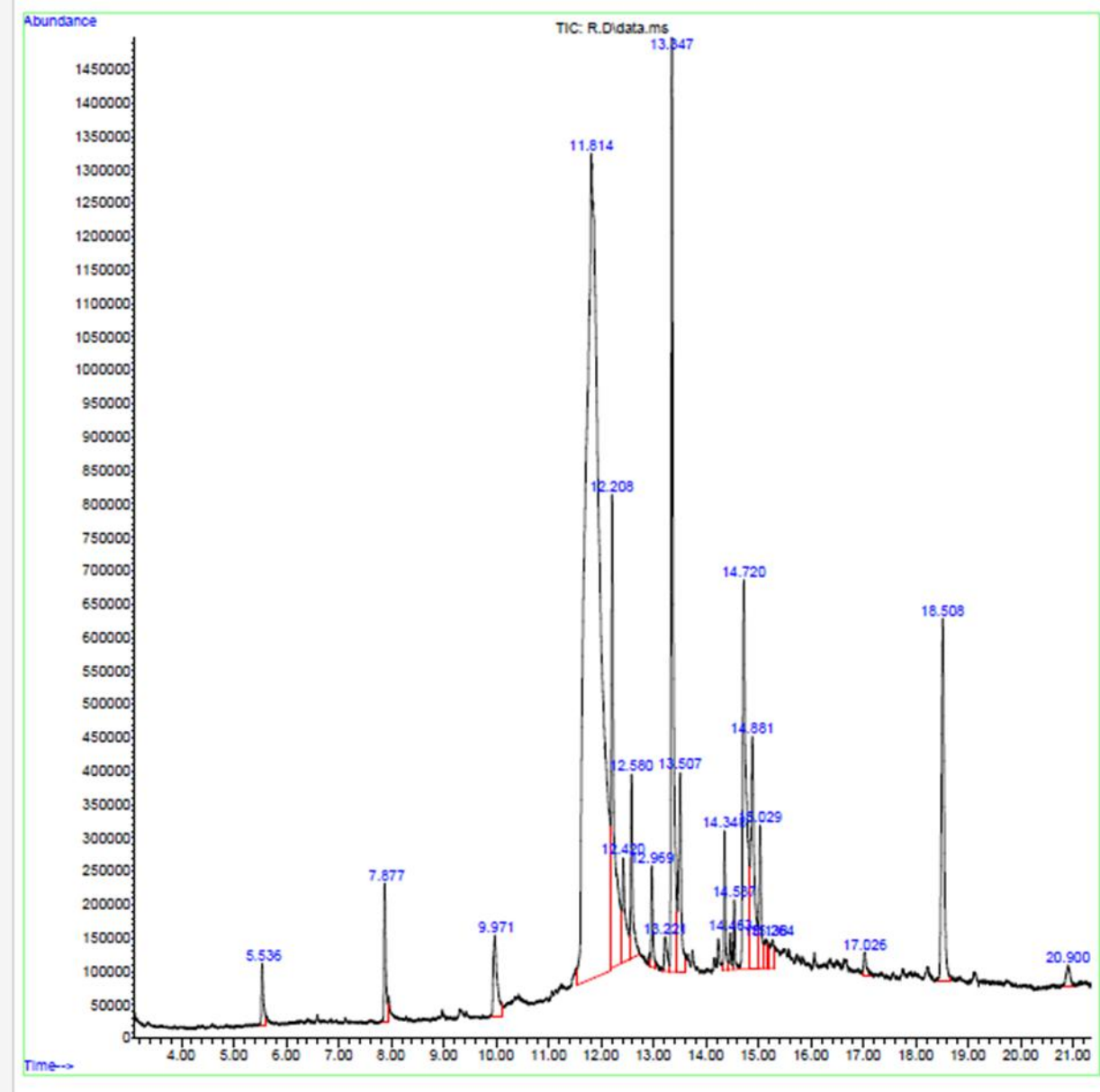

Fig. 6. BT Chromatogram.

Table 3. Constituents of BT stem extract determined from GC-MS

Peak number	Retention time (min)	Compound	% of Total
1	5.536	1-Dodecene	0.59
2	7.877	5-Tetradecene, (E)-	1.10
3	9.971	9-Eicosene, (E)-	1.45
4	11.814	β-d-Mannofuranoside, methyl	54.57
5	12.208	Bicyclo[3.1.1]heptane, 2,6,6-trimethyl-, (1.alpha.,2.beta.,5.alpha.)-	6.31
6	12.420	4-O-Methylmannose	1.50
7	12.580	3,7,11,15-Tetramethyl-2-hexadecen-1-ol	1.73
8	12.969	Pentadecanoic acid, 14-methyl-, methyl ester	0.80
9	13.221	Palmitoleic acid	0.47
10	13.347	n-Hexadecanoic acid	9.49
11	13.507	Hexadecanoic acid, ethyl ester	2.42
12	14.348	9-Octadecenoic acid (Z)-, methyl ester	0.95

13	14.463	7-Oxabicyclo[4.1.0]heptane, 1,5-dimethyl-	0.29
14	14.537	Methyl stearate	0.45
15	14.720	Oleic Acid	6.51
16	14.881	Octadecanoic acid	3.81
17	15.029	Octadecanoic acid, ethyl ester	1.44
18	15.138	cis-Vaccenic acid	0.36
19	15.264	9,12-Octadecadienoic acid (Z,Z)-	0.48
20	17.026	7-Pentadecyne	0.29
21	18.508	Bis(2-ethylhexyl) phthalate	4.61
22	20.900	Undecane	0.36

This compositional variety is beneficial for corrosion inhibition, as plant-derived inhibitors generally function by means of the synergistic adsorption of various constituents onto the metal exterior. The most predominant compound detected is methyl β-D-mannofuranoside, comprising 54.57% of the extract, followed by n-hexadecanoic acid (palmitic acid) at 9.49%, oleic acid at 6.51%, bicyclo[3.1.1]heptane derivatives at 6.31%, and bis(2-ethylhexyl) phthalate at 4.61%. The prevalence of oxygen-rich compounds indicates that the adsorption process on L-CS surfaces in acidic environments is likely facilitated by donor–acceptor interactions. These interactions involve the non-bonded electrons present on heteroatoms and the empty d-orbitals of Fe atoms (El-Housseiny et al., 2022).

In addition, compounds derived from carbohydrates hold particular importance in this context. These molecules contain multiple hydroxyl (–OH) groups, which enhance adsorption through H bonding and coordinate interactions with the metal exterior. In hydrochloric acid environments, such compounds can produce a shielding hydrophilic layer that restricts the diffusion of aggressive chloride ions toward the steel surface, thereby reducing anodic metal dissolution (Khalil et al., 2016; Umoren et al., 2016). The presence of long-chain fatty acids and their esters, including palmitic acid, oleic acid, octadecanoic acid, and their methyl or ethyl esters, further strengthens the inhibitive potential of the BT extract. These compounds possess polar head groups (–COOH or ester functionalities) and non-polar hydrocarbon tails. Unsaturated fatty acids such as oleic and palmitoleic acids are especially effective owing to the existence of pi-electrons in their C=C bonds, which enhance surface interaction through π–d orbital overlap (Elsharif et al., 2020; Khanra et al., 2018). Minor constituents such as alkenes (e.g., 1-dodecene, tetradecene, eicosene) and cyclic hydrocarbons may also contribute to inhibition by increasing surface hydrophobicity once adsorbed. Although present in smaller proportions, their cumulative effect can significantly improve surface coverage (θ) and film stability. The detection of bis(2-ethylhexyl) phthalate, a compound known for strong adsorption tendencies, may also improve the integrity of the adsorbed layer under acidic conditions.
Generally, the inhibitory behavior of BT extract in HCl can be attributed to mixed-type adsorption, involving physical adsorption through electrostatic relations between protonated inhibitor species and the negatively charged L-CS surface, as well as chemical adsorption via electron donation from heteroatoms and π-systems to iron atoms. The high proportion of oxygenated compounds and unsaturated fatty acids supports the establishment of a stable, adherent shielding film, explaining the observed performance of BT for L-CS in HCl.

4. Conclusions

BT stem bark extract exhibits appreciable corrosion inhibition performance for L-CS in 1 M hydrochloric acid. Electrochemical investigations confirm that inhibition efficiency increases with extract concentration, reaching 45% at 1000 ppm from PDP, and 26% from EIS. Dosages higher than 1000 ppm may likely yield higher efficiency of inhibition. The extract functions as a mixed-type inhibitor through adsorption-driven film formation on the steel exterior. The presence of heteroatom-rich organic compounds identified by GC–MS supports the inhibition efficacy of BT. BT stem bark extract exhibited modest performance as an environmental pleasant inhibitor for L-CS corrosion mitigation in HCl. However, the inhibition efficiency exhibited by BT stem bark is low compared to inhibition efficiencies reported for other plant extracts. An enhanced inhibition efficiency could be achieved by utilizing a combination of bark and leaf extracts, or by incorporating other compounds.

CRediT Author Contribution Statement

M. M. Mchihi: Conceptualisation, Supervision, Writing-original Draft, Writing-review & editing.
S. R. Ibukunola: Investigation, Project administration.
B. O. Seriki, P. H. Ado, & A. T. Adejare: Writing-review & editing.
A. O. Eruola & O. S. Olutunji: Formal analysis.

Funding
This research received no external funding.

Conflicts of Interest
The authors declare no conflict of interest.

Acknowledgments

The technical contributions of Dr V. I. Chukwuike of Federal University of Health Science, Uburu, and Dr Ajibaye of Nigerian Institute of Medical Research are acknowledged.

Nomenclature

Symbol	Description	Unit
βa	Anodic tafel slope	$mVdec^{-1}$
βc	Cathodic tafel slope	$mVdec^{-1}$
BT	*Bauhinia tomentosa*	
CPE	Constant phase element	
EIS	Electrochemical impedance spectroscopy	
E_{corr}	Corrosion potential	mV/Ag/AgCl
HCl	Hydrochloric acid	
I_{corr}	Current Density	μAcm^{-2}
IE	Inhibition efficiency	%
L-CS	Low-carbon steel	
n	homogeneity factor	
OCP	Open circuit potential	
PDP	Potentiodynamic polarization	
R_s	Solution resistance	$\Omega\ cm^2$
R_{ct}	Charge transfer resistance	$\Omega\ cm^2$
R_{po}	pore resistance	$\Omega\ cm^2$
θ	Surface coverage	

References

Aldahiri, R. H., Hussein, M. A., Al-Bukhari, S. M., Alamry, K. A., Khan, A., Aslam, R. (2025). Synergistic effect of Canarium strictum leaves extract and KI on the corrosion protection of mild steel in 15% HCl solution. *Scientific Reports, 15*, 3576. https://doi.org/10.1038/s41598-025-87482-x

Al-Moubaraki, A. H., Chaouiki, A., Alahmari, J. M., Al-hammadi, W. A., Noor, E. A., Al-Ghamdi, A. A., Ko, Y.G. (2022). Development of Natural Plant Extracts as Sustainable Inhibitors for Efficient Protection of mild steel: Experimental and First-Principles Multi-Level Computational Methods. *Materials*, *15*, 8688. https://doi.org/10.3390/ma15238688

El-Housseiny, S., Abdel-Gaber, A. M., Rahal, H.T., Beqai, F.T. (2022). Eco-friendly corrosion inhibitor for mild steel in acidic media. *International Journal of Corrosion and Scale Inhibition*, *11*(4), 1516–1538. 10.17675/2305-6894-2022-11-4-6

Eddy, N. O., Momoh-Yahaya, H., Oguzie, E. E. (2015). Theoretical and experimental studies on the corrosion inhibition potentials of some purines for aluminum in 0.1 M HCl. *Journal of Advanced Research*, *6*, 203–217. http://dx.doi.org/10.1016/j.jare.2014.01.004

Balabhaskar, R. Vijayalakshmi, K. (2015) Preliminary phytochemical and pharmacognostic analysis of Bauhinia tomentosa. *Journal of Chemical and Pharmaceutical Research*, *7*(4), 271-277.

Chioma, F., Odozi, N. W. Mchihi, M. M., Olatunde, M. A. (2022). Synthesis, spectroscopic, and density functional theory studies of the corrosion inhibitive behaviour of *n*-(1,4-dihydro-1,4-dioxonaphthalene-3-yl)pyrazine-2-carboxamide chelator-ligand. *Global journal of pure and applied sciences, 28*, 39-50. https://dx.doi.org/10.4314/gjpas.v28i1.6

Chu, T.-S., Mai, W.-J., Li, H.-Z., Wei, B.-X., Xu, Y.-Q., Liao, B.-K. (2025). Insights into the Corrosion Inhibition Performance of Plant Extracts of Different Genera in the Asteraceae Family for Q235 Steel in H_2SO_4 Medium. *International Journal of Molecular Sciences, 26*, 561. https://doi.org/10.3390/ijms26020561

Emesiani, M. C., Umegbolu, V. C., Mchihi, M. M. (2024). Corrosion inhibitory attributes of mixture of codiaeum variegatum and *Ficus benhamina* for mild steel in hydrochloric acid medium. *FUDMA Journal of Sciences 8*(3), 258 - 263. https://doi.org/10.33003/fjs-2024-0805-2677.

Elsharif, A. M., Abubshait, S. A., Abdulazeez, I., Abubshait, H. A. (2020). Synthesis, characterization and corrosion inhibition studies of polyunsaturated fatty acid derivatives on the acidic corrosion of L-CS: Experimental and computational studies. *Journal of Molecular Liquids, 319*, 114162. https://doi.org/10.1016/j.molliq.2020.114162

Fazal, B. R., Becker, T., Kinsella, B., Lepkova, K. (2022). A review of plant extracts as green corrosion inhibitors for CO_2 corrosion of carbon steel. *Materials degradation 6*(5). https://doi.org/10.1038/s41529-021-00201-5

Gerengi, H., Sahin, H. I. (2012). Schinopsis lorentzii Extract As a Green Corrosion Inhibitor for Low Carbon Steel in 1 M HCl Solution. *Industrial & Engineering Chemistry Research 51*, 780–787. dx.doi.org/10.1021/ie201776q

Ituen, E., James, A., Akaranta, O. & Sun, S.(2016). Eco-friendly corrosion inhibitor from Pennisetum purpureum biomass and synergistic intensifiers for mild steel. *Chinese Journal of Chemical Engineering, 24*, 1442–1447.

Khalil, S. M., Al-Mazaideh, G. M., Ali, N. M. (2016). DFT Calculations on Corrosion Inhibition of Aluminum by Some Carbohydrates. *International Journal of Biochemistry Research & Review, 14*(2), 1–7. https://doi.org/10.9734/IJBCRR/2016/29288.

Khanra, A., Srivastava, M., Rai, M. P., Prakash, R. (2018). Application of Unsaturated Fatty Acid Molecules Derived from Microalgae toward L-CS Corrosion Inhibition in HCl Solution: A Novel Approach for Metal–Inhibitor Association. *ACS Omega*, *3*(10), 12369–12382. https://doi.org/10.1021/acsomega.8b01089

Kumar, S. P., Aditya, S., Pal, S. J., Mukesh, K. (2025). Bauhinia tomentosa L.: A Comprehensive Review of Its Ethnopharmacology, Phytochemistry, and Therapeutic Medicinal Values. *Journal of Medicinal Natural Products*, *2*(3), 100016. https://doi.org/10.53941/jmnp.2025.100016

Mahraz, M. A, Salim, R., Loukili, H., Laftouhi, A., Haddou, S., Elrherabi, A., Bouhrim, M., Herqash, R. N., Shahat, A. A., Eto, B., Hammouti, B., Rais, Z., Taleb, M. (2025). Ephedra fragilis plant extract: A groundbreaking corrosion inhibitor for mild steel in acidic environments-electrochemical, EDX, DFT, and Monte Carlo studies. *Open life sciences*, *20*, 20221050. https://doi.org/10.1515/biol-2022-1050

Meena, O., Kausha, S., Kumar, S., Dalal, J. (2024). *Euphorbia neriifolia* extracts as green corrosion inhibitor for aluminium in hydrochloric and nitric acid media. *Discover materials, 4*, 102. https://doi.org/10.1007/s43939-024-00157-8

Mchihi, M. M., Emesiani, M. C., Babawumi, J. I. (2023). Inhibitory Potentials of Leaf Extract of *Justicia schimperi* for Mild Steel Corrosion in Hydrochloric Acid Medium: Gravimetric, Microscopic and Spectroscopic Studies. *Asian Research Journal of Current Science, 5*(1), 184-192.

Mchihi, M. M., Odozi, N. W., Odimuko, A. B. (2025a). Deciphering properties of *Dryopteris marginalis* as green corrosion inhibitor for mild steel in HCl: Electrochemical, gas chromatography and DFT studies. *Sustainable Chemistry One World*, *7*, 100103. https://doi.org/10.1016/j.scowo.2025.100103

Mchihi, M. M., Olatunde, A. M., Odozi, N. W. (2025b). CuO-based nanocomposite: synthesis, characterization, and evaluation of the corrosion inhibition effectiveness for mild steel in HCl. *Journal of Electrochemical Science and Engineering, 15*(4)*,* 2715. https://doi.org/10.5599/jese.2715

Mchihi, M. M., Olatunde, A. M., Odozi, N. W. (2025c). Electrochemical and Gravimetric Studies of the Corrosion Inhibitory P roperties of Green Synthesized Copper Oxide Nanoparticles Mediated by *Ficus sur* for Mild Steel in HCl. *Jordan Journal of Chemistry*, *20*(2), 81-93. https://doi.org/10.47014/20.2.1

Mchihi, M. M., Odozi, N. W., Gbolahan, S. A. (2024a). Electrochemical investigation of the inhibitory effect of zinc oxide nanoparticles/tenofovir disoproxil fumarate nanocomposite on mild steel corrosion in 1 M hydrochloric acid. *Analytical and Bioanalytical Electrochemistry*, *16*(6), 559-567. https://doi.org/10.22034/abec.2024.714079

Mchihi, M.M., Odozi, N.W., Nurudeen, A.O., Emesiani, M.C., Seriki, B. O. (2024b). Assessment of *Helianthus tuberosus* leaves extract as eco-friendly corrosion inhibitor for Aluminum in sodium hydroxide: Insights from electrochemical, gravimetry and computational consideration. *Moroccan Journal of Chemistry*, *12*(4), 1462-1483. https://doi.org/10.48317/IMIST.PRSM/morjchem-v12i4.49160

Mchihi, M. M., Olatunde A. M., Odozi, N. W. (2024c). *Ficus sur* mediated synthesis of mesoporous ZnO nanoparticles and novel ZnO/Arginine/Tyrosine nanocomposite as eco-friendly corrosion inhibitors for mild steel in hydrochloric acid medium. *Moroccan Journal of Chemistry*, *12*(3), 1122-1152. https://doi.org/10.48317/IMIST.PRSM/morjchem-v12i3.42782

Miralrio, A., Vázquez, A. E. (2020). Plant Extracts as Green Corrosion Inhibitors for Different Metal Surfaces and Corrosive Media: A Review. *Processes 8*, 942. https://doi.org/10.3390/pr8080942

Mungwari, C. P., Obadele, B. A., King'ondu, C. K. (2025). Phytochemicals as green and sustainable corrosion inhibitors for mild steel and aluminium: Review. *Results in Surfaces and Interfaces, 18*, 100374. https://doi.org/10.1016/j.rsurfi.2024.100374

Nnanna, L. A. Onwuagba, B. N., Mejeha, I. M., Okeoma, K. B. (2010). Inhibition effects of some plant extracts on the acid corrosion of aluminium alloy. *African Journal of Pure and Applied Chemistry, 4*(1), 011-016.

Obiukwu, O., Opara, I., Grema, L. U. (2015). Corrosion Inhibition of Mild Steel by Various Plant Extracts in Acid Media. *Research Journal of Applied Sciences, Engineering and Technology, 10*(10) 1197-1205. 10.19026/rjaset.10.1888

Odozi, N. W., Adetoba, A. S., Mchihi, M. M. and Akpaetok, A. N. (2021). *Synsepalum dulcificum* leaves extract as green inhibitor for mild steel corrosion in hydrochloric acid. *ChemSearch Journal, 12*(1), 47 – 54. http://www.ajol.info/index.php/csj

Odozi, N. W., Emesiani, M. C., Charles, C. D., Seriki B. O., Mchihi M. M. (2024). Electrochemical studies of the corrosion inhibitory potential of *Annona muricata* leaves extract on aluminum in hydrochloric acid medium. *FUDMA Journal of Sciences, 8*(3), 395 - 401. https://doi.org/10.33003/fjs-2024-0803-2460

Odozi N.W., Saheed R., Mchihi M. M. (2019). Application of *peperomia pellucida* leaves extract as a green corrosion inhibitor for mild steel in 1.0 M hydrochloric acid solution. *Chemsearch journal, 10*(2), 88 – 93. http://www.ajol.info/index.php/csj

Perumal, S., Muthumanickam, S., Elangovan, A. Karthik, R. Sayee kannan, R., Mothilal, K. K. (2017). Bauhinia tomentosa Leaves Extract as Green Corrosion Inhibitor for mild steel in 1M HCl Medium. *Journal of Bio- and Tribo- Corrosion, 3*, 13. https://doi.org/10.1007/s40735-017-0072-5

Rani, A.T.J., Thomas, A., Arshad, M., Joseph, A., (2022). The influence of aqueous and alcoholic extracts of Garcinia Cambogia fruit rind in the management of mild steel corrosion in hydrochloric acid: theoretical and Electroanalytical Studies. *Journal of Molecular Liquid, 346*. https://doi.org/10.1016/j.molliq.2021.117873.

Rathod, M.R., Minagalavar, R.L., Rajappa, S.K., (2022). Effect of artabotrys odoratissimus extract as an environmentally sustainable inhibitor for mild steel corrosion in 0.5 M H_2SO_4 media. *Journal of the Indian Chemical Society, 99*(5), 100445. https://doi.org/10.1016/j.jics.2022.100445.

Thacker, H., Ram, V. (2025). Green corrosion inhibitors derived from plant extracts and drugs for mild steel in acid media: A review. *Results in Surfaces and Interfaces 18*, 100364. https://doi.org/10.1016/j.rsurfi.2024.100364

Umoren, S. A., Eduok, U. M. (2016). Application of carbohydrate polymers as corrosion inhibitors for metal substrates in different media: A review. *Carbohydrate Polymers*, *140*, 314-341. https://doi.org/10.1016/j.carbpol.2015.12.038

Verma, C., Alrefaee, S. H., Quraishi, M. A., Ebenso, E. E., Hussain, C. M. (2021). Recent developments in sustainable corrosion inhibition using ionic liquids: A review. *Journal of Molecular Liquids*, *321*, 114484. https://doi.org/10.1016/j.molliq.2020.114484

Zheng, X., Gong, M., Li, Q. & Guo, L. (2018). Corrosion inhibition of mild steel in sulfuric acid solution by loquat (Eriobotrya japonica Lindl.) leaves extract. *Scientific Reports, 8*, 9140. https://doi.org/10.1038/s41598-018-27257-9